OPTICAL PROPERTIES AND THE DETECTION OF BLOWING SNOW

J.W. Pomeroy and D.H. Male

Division of Hydrology
University of Saskatchewan
Saskatoon, Saskatchewan
Canada S7N OWO

Paper prepared for: "Symposium on Remote Sensing and Electromagnetic Properties of Snow and Ice"

American Geophysical Union Fall Meeting
11 December 1985
San Francisco, California, U.S.A.

OPTICAL PROPERTIES AND THE DETECTION OF BLOWING SNOW

J.W. Pomeroy and D.H. Male

INTRODUCTION

A characteristic of blowing snow is reduced visibility caused by the ability of snow particles to scatter and absorb electromagnetic radiation. Several empirical investigations of the light extinguishing characteristics of blowing snow have been published (Landon-Smith and Woodberry, 1965; Mellor, 1966; Tabler, 1984) which suggest that this property can be used to measure the mass of blowing snow per unit volume of atmosphere (drift density). Recent investigations of falling snow (Seagraves, 1984) suggest that both the snow crystal size distribution and mass concentration of falling snow can be measured using the light extinction properties of snow.

It is the purpose of this study to examine the optical properties of blowing snow for the visible and infrared wavelengths and to demonstrate the application of these properties in the calibration of an optical measuring system for blowing snow. Schmidt et al. (1984) have demonstrated that optical measuring systems are capable of rapid, continuous measurements with minimal interference to the snow-air flux. A theoretically calibrated system capable of measuring both the particle size distribution and drift density has an advantage over empirically calibrated mass flux traps.

PROPERTIES OF BLOWING SNOW

Blowing snow is surface snow which has been entrained and is being transported by the wind. The mode of transport within about 0.05 m of the surface is saltation, which involves regular momentum exchange between the particle and the snow surface as well as the horizontal component of the wind. Above about 0.05 m, suspended transport occurs, and has been observed at heights up to 1000 m in Western Canada. The fall velocities of blowing snow particles are in the same range as vertical turbulent velocities during blowing snow. As a result there

is an exponential decrease in the drift density as height is increased.

Blowing snow particles are usually metamorphosed fragments of the surface snow cover and bear little similarity to falling snow crystals. The snow fragments are abraded during saltation and rapidly become rounded, though occasionally somewhat ellipsoid (Schmidt, 1981). During suspended transport, enhanced sublimation further rounds and smooths the particles. The density of blowing snow particles is approximately equal to that of ice. Thus blowing snow particles approach the "optically ideal" ice sphere more closely than do other forms of snow.

The size distribution of blowing snow particles has been fitted to the two parameter gamma distribution for both suspended (Budd, 1966) and saltating transport modes (Schmidt, 1981; 1984). This distribution has the form

$$f(P_r) = \frac{P_r^{(\alpha-1)} \, e^{(-P_r/\beta)}}{\beta^{\alpha} \, \Gamma_{(\alpha)}} \quad , \qquad (1)$$

where $f(P_r)$ is the relative frequency of particle radius P_r, α is the distribution shape parameter, β is the scale parameter and Γ denotes a gamma function. The parameters α and β are also defined in terms of the mean particle radius $\overline{P_r}$ (Haan, 1977) where

$$\overline{P_r} = \alpha\beta \quad . \qquad (2)$$

The value of α is approximately 5 for saltating and 10 for suspended transport. The mean particle radius decreases with height, typical values being 100 μm near the surface and 40 μm at 2 m. The degree of turbulence in the wind can cause $\overline{P_r}$ to fluctuate for a given height.

OPTICAL PROPERTIES OF BLOWING SNOW

The electromagnetic transmittance through a dispersive media is the ratio of the light intensity transmitted through the media to that intensity transmitted without the scattering and absorption effects of the media. Following the

Bouger-Lambert law, the transmittance T through an ensemble of small particles is found from the length of transmission L and the extinction coefficient σ_λ for the wavelength λ considered, where

$$T = e^{(-\sigma_\lambda L)} \quad . \tag{3}$$

The extinction coefficient is a function of the cross-sectional area of particles per unit volume and the extinction efficiency Q_e of the particles. Thus,

$$\sigma_\lambda = \pi N \int_{P_r} f(P_r)\ P_r^2\ Q_e\ (P_r,\lambda) dP_r \quad . \tag{4}$$

In Eq. 4 N is the number of particles per unit volume of atmosphere, and $\int_{P_r} dP_r$ denotes the integral of P_r over the radius range.

The extinction coefficient can be expressed in terms of the drift density η by the following substitution. The drift density is defined as

$$\eta = 4/3\ \pi\rho_i\ N \int_{P_r} f(P_r)\ P_r^3\ dP_r \quad , \tag{5}$$

where ρ_i is the density of snow particles. Substituting the drift density into Eq. 4 and integrating over the particle radius yields

$$\sigma_\lambda = \frac{3\eta \int_{P_r} Q_e(P_r,\lambda)\ P_r^{(\alpha+1)}\ e^{(-P_r/\beta)}\ dP_r}{4\rho_i\ (\alpha+2)!\ \beta^{(\alpha+3)}} \quad . \tag{6}$$

Thus, the extinction coefficient is a function of η, α, β and λ.

The variation of Q_e with P_r and λ must be defined to solve Eq. 6. In classical geometrical optics Q_e is considered equal to 2.0, an approximation which is only valid for particles that are large with respect to the light wavelength. For smaller particles Q_e is a function of the particle size parameter $x = 2\pi P_r/\lambda$ and the complex index of refraction. This function can be calculated using the Mie complex angular momentum approach to light scattering (van de Hulst, 1957). However, even the fastest algorithms (Wiscombe, 1980;

Ungut et al., 1981) can require excessive computing time, particularly when x is large and a range of scattering angles and size parameters are considered. Nussenzveig and Wiscombe (1980) have proposed asymptotic approximations to the extinction efficiency based on Mie theory. These calculations exhibit errors of less than 0.01% when compared to exact Mie calculations and are well suited to applications where an ensemble of non-uniform particles are considered.

Blowing snow particles are essentially ice spheres, for which Irvine and Pollack (1968) have calculated the real and imaginary components of the index of refraction for various wavelengths. Using these values, the extinction efficiency Q_e has been calculated using Nussenzveig and Wiscombe's (1980) algorithm. The results are plotted against the snow particle radius for various wavelengths in Fig. 1. Note that for λ = 300 nm, Q_e is within 1% of 2.0 for particles greater than 50 μm in radius. The corresponding radii for which Q_e is within 1% of 2.0 for λ = 600 nm is 95 μm and for λ = 1.06 μm is 168 μm. Q_e at λ = 2 μm is never consistently within 1% of 2.0. For blowing snow, the difference between the geometrical optics and Mie theory Q_e becomes more pronounced as wavelength increases and extends to larger particle sizes. However, at all wavelengths, the smaller particles exhibit greater extinction efficiencies than do larger particles.

The behaviour of the extinction coefficient can be demonstrated by its effect on the meteorological visual range, an inverse linear function of σ_λ. The meteorological visual range V is the maximum distance at which an "average" eye can distinguish a black object of 1° in visual angle. Koschmieder's definition of visual range at a given wavelength (Middleton, 1952) is;

$$V_\lambda = 3.912/\sigma_\lambda \quad . \tag{7}$$

While the concept of "visual" range becomes abstract outside of the visible spectrum, it is a standard meteorological variable and a useful surrogate for the extinction coefficient.

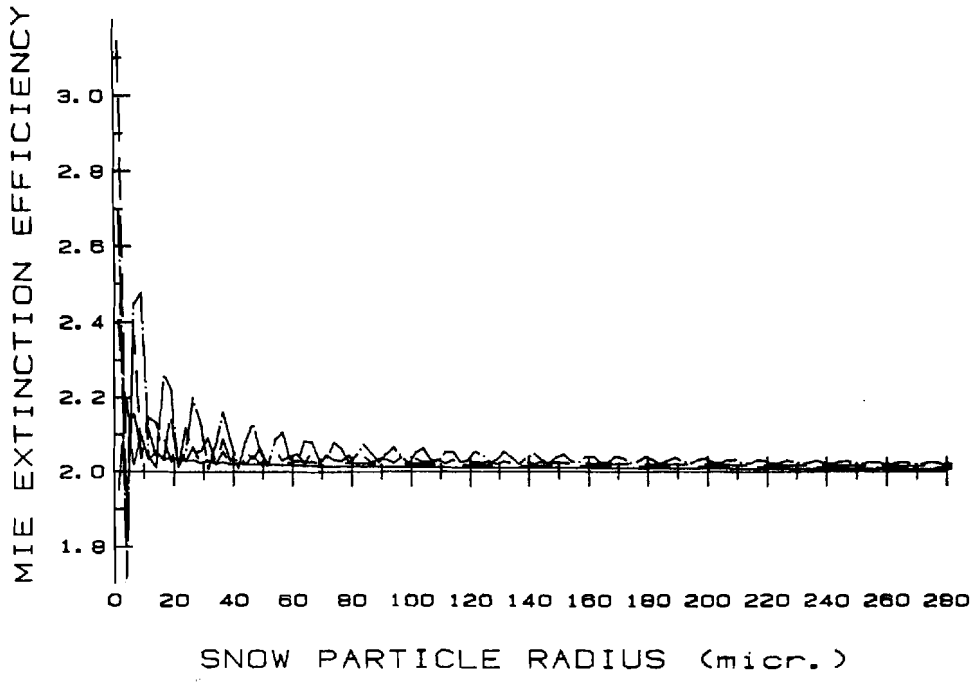

Figure 1. Mie Extinction Efficiencies. Calculated for blowing snow using Nussenzveig and Wiscombe's (1980) asymptotic approximation for wavelengths of 300 nm ———, 600 nm ----, 1.06 μm — — — and 2.0 μm — · —. The geometrical optics approximation is 2.0.

Calculation of V_λ involves combining Eqs. 6 and 7, defining the particle size distribution parameters and solving for various wavelengths and drift densities. Budd (1966) and Schmidt (1982) suggest for suspended blowing snow particle radii that $\alpha = 10$ is a reasonable value. Pomeroy et al. (1985) demonstrate that for a given $\overline{P_r}$, even a 50% variation in α results in an insignificant change in σ when integrated over the particle size distribution. The visual range through blowing snow as a function of drift density for $\alpha = 10$, a variety of λ and the suspended range of $\overline{P_r}$ has been calculated and is plotted in Fig. 2. Variation in wavelength from the ultraviolet to near infrared results in a visual range variation of between 1.5 to 8.3% with other factors constant. However, variation of the mean particle radius through its range for suspended blowing snow results in visual range variation of between 52.9 and 56.2% with other factors constant. The mean particle size appears to be an important factor affecting the blowing snow drift density - visual range relationship.

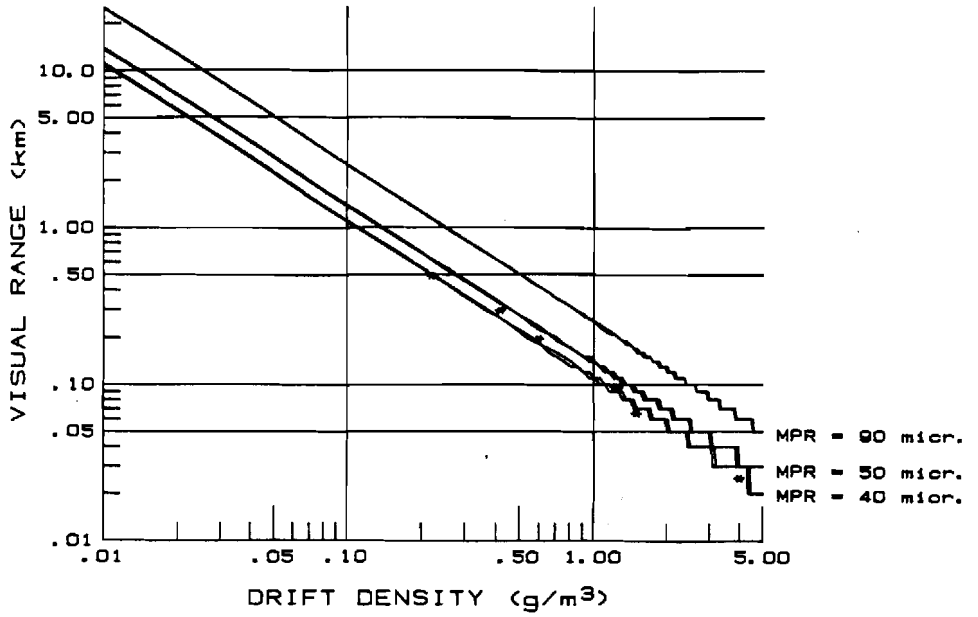

Figure 2. Visual Range in Blowing Snow. Calculated for a gamma distribution of particle radii α of 10, $\overline{P_r}$ of 40, 50 and 90 μm and wavelengths of 300, 600, 1006 and 2000 nm though the wavelengths are not individually discernable. Budd et al.'s (1966) observations are plotted as *.

Meteorological visual ranges (visible spectrum) and drift densities at a 2-m height were measured in the Antarctic by Budd et al. (1966). These data are also plotted in Fig. 2 and correspond to the theoretical predictions using $\overline{P_r}$ = 40 μm. While Budd et al. (1966) do not provide the $\overline{P_r}$ value from their observations, Budd (1966) indicates an expected $\overline{P_r}$ of 40-45 μm at a 2-m height for similar conditions. The data of Budd et al., while sparse, agrees well with the results of the theoretical model.

OPTICAL DETECTION OF BLOWING SNOW

The wavelength and particle size dependence of the drift density-extinction coefficient relationship suggests at least two approaches to the detection of blowing snow properties. One approach involves measuring the transmittance through blowing snow with opto-electronic detectors at two widely separated wavelengths and then solving for both the drift density and β from the particle size distribution. Another approach involves measuring the time averaged

transmittance of an ensemble of particles with a wide beam detector and counting individual particles with a narrow beam detector. Our objective of an inexpensive and reliable field component could not be met by the first approach, as detectors sensitive to 6-12 μm wavelengths are both expensive and difficult to maintain in the field. The second approach uses detectors and sources which are commonly used in the fibre-optics communications industry. We chose the second approach and detail it here.

The Division of Hydrology extinction meter (wide beam detector) uses a photodiode detector of 1300 μm radius mounted 0.15 m from a collimated LED source of equivalent diameter. The detector and LED are spectrally matched, with a peak wavelength of 900 nm, to reduce the relative intensity of ambient light. The LED is modulated to allow further compensation for ambient light levels. The extinction meter measures light intensity, which is referenced to the unattenuated intensity to provide the transmittance and following Eq. 3, the extinction coefficient. For detectors whose angular radius with the particle is greater than $\sim 0°$, the extinction efficiency must be corrected for forward scattering of light into the detector. These corrections can be made by calculating forward scattering intensities using the Mie theory for a range of angular radii defined by the possible particle positions in the beam and the detector radius. However, computational times (Wiscombe, 1980) are excessive. van de Hulst (1957), Hodkinson and Greenleaves (1963) and Ungut et al. (1981) have shown that full geometrical optics approximations can be used for accurate light scattering computations, especially when forward angles are less than 20° and a range of wavelengths and particle sizes are used. These approximations are valid for the index of refraction, wavelength and range of particle sizes used in this application.

The extinction efficiency, Q_e, as calculated using the method of Nussenzveig and Wiscombe (1980) is corrected for forward scattering from Fraunhoffer diffraction

and refraction without internal reflection. Pomeroy et al. (1985) have shown that forward scattering from externally reflected light is less than 0.1% of received intensities in blowing snow. The diffraction correction ΔQ_d to Q_e accounts for light diffracted forward by the particle into a solid angle defined by the detector radius D_r and distance ℓ from particle to detector. Hodkinson and Greenleaves (1963) present a formula for ΔQ_d based on the work of van de Hulst (1957). This formula is integrated over the detection distance L to provide a spatially averaged correction

$$\Delta Q_d = 1 - \int_o^L (J_o^2[x \sin(D_r/\ell)] - J_1^2[x \sin(D_r/\ell)]d\ell \quad , \tag{8}$$

where $x = 2\pi P_r/\lambda$ and J_o and J_1 are zeroth and first order Bessel functions of the first kind respectively. For the extinction meter, the magnitude of ΔQ_d can be 50% of Q_e and increases with particle size.

The refraction correction ΔQ_r is a function of the complex index of refraction m and the particle detector geometry. The formula presented by Hodkinson and Greenleaves (1963) is integrated over the detection distance to give

$$\Delta Q_r = 4\left(\frac{m}{m^2-1}\right)^4 \int_o^\theta \frac{(mA-1)^3(m-A)^3(1+B)C}{A(m^2+1-2mA)^2} d\theta \quad , \tag{9}$$

where $A = \cos\theta/2$, $B = \sec^4\theta/2$, $C = \sin\theta$ and $\theta = \arcsin(D_r/\ell)$. In practise a simplified expression can be fit to the results of Eq. 9 once the index of refraction has been selected. For the extinction meter the magnitude of ΔQ_r is less than 1% of Q_e and is independent of particle size.

The effective extinction efficiency Q_{ef} is the Mie approximation Q_e corrected for forward scattering and is a function of the detector geometry and the refractive qualities of the light dispersive media. Thus

$$Q_{ef} = Q_e - \Delta Q_d - \Delta Q_r \quad . \tag{10}$$

Q_e and Q_{ef} are plotted as functions of the snow particle radius for the extinction meter configuration in Fig. 3. There is a dramatic drop in the effective

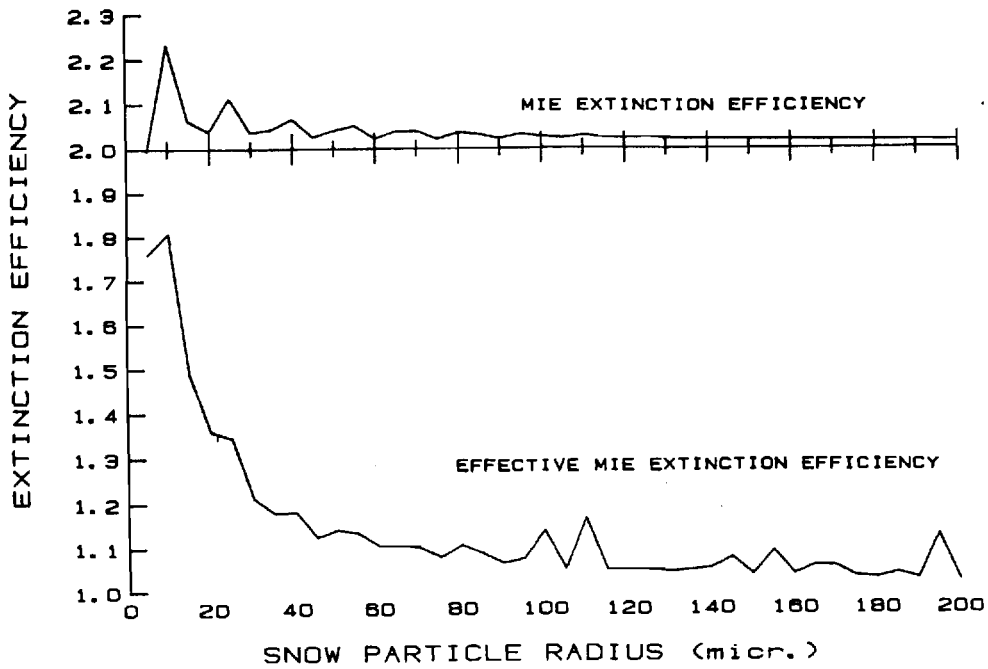

Figure 3. Extinction Efficiencies for the Extinction Meter. The Mie extinction efficiency and effective extinction efficiency corrected for diffraction and refraction are calculated for the Division of Hydrology Extinction Meter.

extinction efficiency as the particle radius increases from 15 to 50 μm. In terms of geometrical optics, for larger particles almost all of the diffracted component of scattered light is scattered forward into the detector. While this feature reduces the sensitivity of the gauge, the effect of the particle size distribution on the extinction coefficient will be greater than for the visual range case.

The performance of the extinction meter can be modelled using Eqs. 3, 6, 8, 9 and 10 and substituting Q_{ef} for Q_e. The results are shown in Fig. 4. A variation in the mean snow particle radius through its normal range can result in transmittance differences of 0.35 for a constant drift density. This behaviour necessitates the determiniation of the particle size distribution to calibrate the transmittance - drift density relationship. However, the variation with particle size provides a tool for indirect measurement of the size distribution.

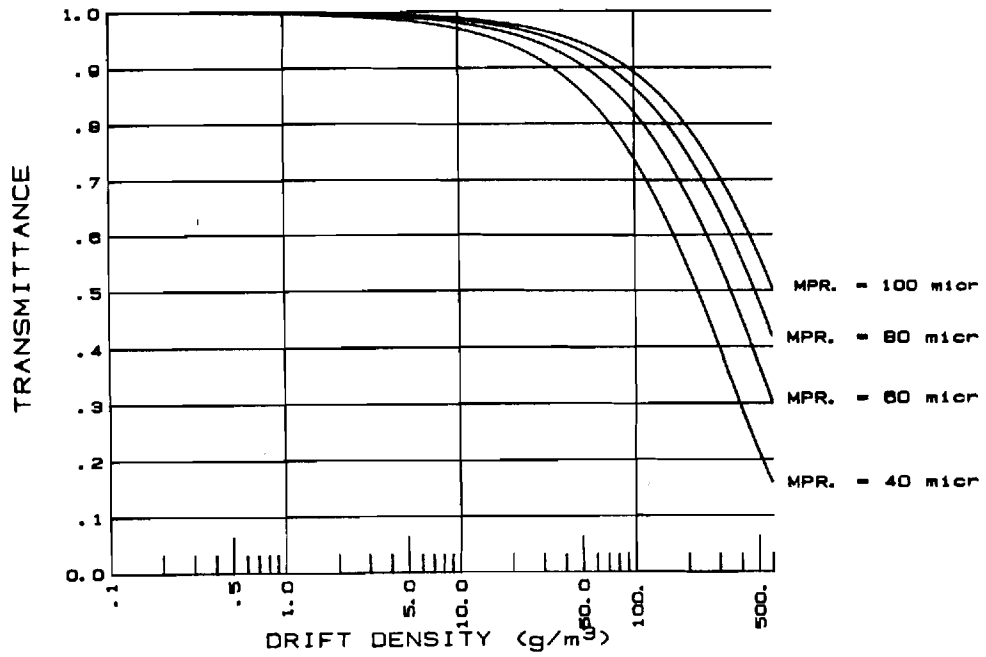

Figure 4. Extinction Meter Performance. Transmittance calculated for a gamma distribution of aprticle radii α of 10 and $\overline{P_r}$ of 40, 60, 80 and 100 μm.

The Division of Hydrology particle detector (narrow beam detector) uses a photodiode detector of 150 μm radius mounted 0.02 m from a collimated LED source of equivalent diameter. The peak wavelength of transmission for this system is 820 nm. The particle detector counts the number of particles per second whose individual transmittances drop beyond the threshold level for detection. The transmittance, T, associated with a single particle intercepting a collimated light beam is calculated following Zuev (1970). Thus

$$T = T_o - (I_r^2/D_r^2)\, Q_{ef} \quad , \tag{11}$$

where T_o is the transmittance antecedent to the beam interception, I_r is the intercepted radius of the particle and D_r is the radius of the detector (and beam). The intercepted particle radius is the radius of a circle of equivalent area to that area of the particle which is intercepted by the beam. It is a function of both the particle radius and the cross-sectional trajectory of the particle through the beam.

The effective extinction efficiency as a function of the intercepted particle radius is calculated for the particle detector in the same manner as for the extinction meter. The results for the particle detector configuration are plotted in Fig. 5. Most of the diffracted light from particles with I_r greater than 60 μm is scattered forward into the detector. The effect of interference phenomena between various orders of scattering rays is expressed in the inconsistency in Q_{ef} for radii above 70 μm.

The transmittance associated with an intercepted particle radius and the variation in this transmittance with a particle crossing position between source and detector can be examined by calculating Q_{ef} without integrating over distance from the detector (see Eqs. 8 and 9). This $Q_{ef}(\ell)$ is horizontally specific as opposed to the integrated Q_{ef} plotted in Fig. 5. Using Eq. 11, the transmittance is calculated as a function of I_r and ℓ and the results plotted in Fig. 6. The particles have greater light extinguishing effects as distance increases from the detector. Inconsistencies in some values of T result from diffraction interference effects which appear more severe when not averaged out as in Fig. 5. These effects are less prominent when incoherent light and a range of particle sizes are considered.

If the threshold transmittance of detection for the particle detector was 1.0 and the particle radius much less than the beam radius, then the number of snow particles per unit volume of atmosphere N could be determined from the number of particles counted per second, ϕ, the sampling area of the beam perpendicular to the particle flux, A_s, and the horizontal particle speed which is equivalent to the horizontal wind speed, u, where

$$N = \phi/uA_s \quad . \tag{12}$$

However, because the light beam is relatively narrow, the sampling area differs for each particle size and is a function of the vertical deviation of particle trajectories from the beam centre for which I_r is greater than some threshold.

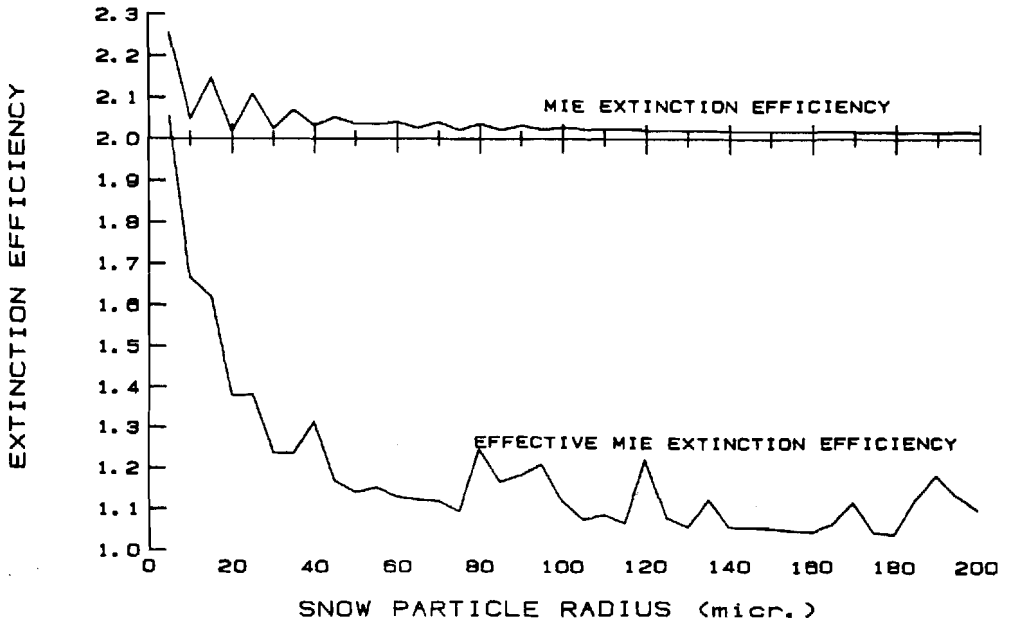

Figure 5. Extinction Efficiencies for the Particle Detector. The Mie extinction efficiency and effective extinction efficiency corrected for diffraction and refraction are calculated for the Division of Hydrology Particle Detector.

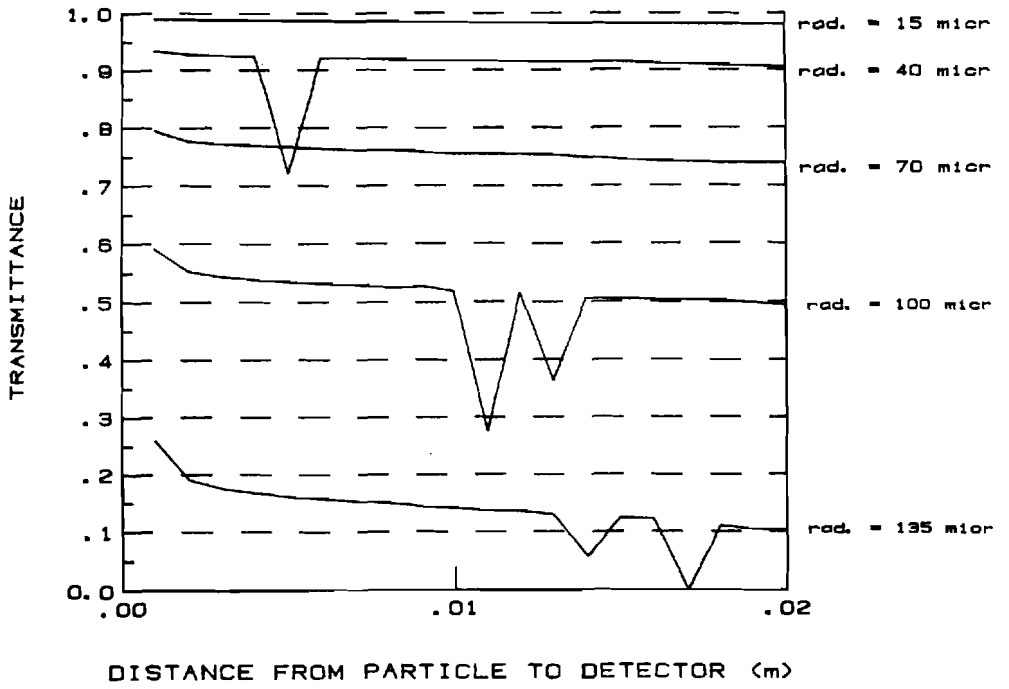

Figure 6. Single Particle Extinction for the Particle Detector. Transmittance calculated for single particles of 15, 40, 70, 100 and 135 μm radius at various distances from the detector.

A complete discussion of techniques for calculating A_s from the particle and beam geometries is included in Pomeroy et al. (1985).

Because of background electronic noise levels and high particle speeds ($\sim$ 15 m/s) actual threshold transmittances of detection are intrinsic to individual detectors and range from 0.90 to 0.995. A threshold radius is defined as the intercepted radius which results in a horizontally averaged transmittance at the threshold of detection. Figure 6 shows that the errors in using the mean transmittance become small as a transmittance of 1.0 is approached. Equation 12 is modified to account for this threshold radius by dividing the number density of particles greater than the threshold for detection by the cumulative frequency of particles greater than this threshold. To account for sampling areas specific to each P_r, the frequency of each P_r is divided by the sampling area for that radius. Using the gamma distribution, the resulting form of the equation is

$$N = \frac{\phi \int_{P_{tr}}^{\infty} [P_r^{(\alpha-1)} e^{(-P_r/\beta)} / A_s(P_r)] dP_r}{u \int_{P_{tr}}^{\infty} P_r^{(\alpha-1)} e^{(-P_r/\beta)} dP_r} \quad . \qquad (13)$$

In Eq. 13 $A_s(P_r)$ is the sampling area for particles of radius P_r and P_{tr} is the particle radius at the threshold detection (when $I_r = P_r$). Equation 13 can be substituted into Eq. 4 and with the extinction coefficient known from the extinction meter and α assumed a constant, β can be found. With β known, a form of Eq. 6 can be precisely solved for the drift density.

Thus the inputs for this blowing snow measuring system are an assumed α, the extinction coefficient from the extinction meter, the number of particles counted per second by the particle detector and the mean windspeed at the height of detection. Outputs of the system are the drift density of blowing snow, the size distribution of snow particles and the product ηu which is the mass flux of blowing snow.

CONCLUSIONS

Calculation of the Mie extinction efficiencies for blowing snow particles shows the classical geometrical optics approximation of $Q_e = 2.0$ is not valid for particle radii less than 50 μm in the near ultraviolet and less than 95 μm in the middle visible range. The geometrical optics approximation is not valid at all for the normal range of blowing snow particle radii when wavelengths in the near infrared are used. Since Q_e can range above 2.5 for particle radii less than 15 μm in visible and near infrared wavelengths, use of Mie approximations to calculate the extinction efficiency is recommended.

The visible range - drift density relationship is inverse and logarithmic. However, the relationship is almost linear for the range of drift densities from 0.01 to 0.1 g/m^3 for which the visible range drops from approximately 15 to 1.5 km. This helps to explain the low visibilities frequently experienced at "eye" level during snow storms, despite the relatively low drift densities found at the 1.5 to 2.5 m heights. A range of wavelengths from 300 to 2000 nm produces a relatively small change in the visible range, no wavelength possessing clearly superior light transmission characteristics in this range. However, variation in the particle size distribution over its blowing snow range produces significant effects on the visibility with approximately 55% change over the range of mean particle radii. The smaller particles exhibit lower visible ranges. These particles predominate at eye level, another factor in low visibilities at this height.

The correction required to the extinction efficiency for forward scattering of diffracted light into the detectors is significant, being approximately 50% reduction in Q_e for larger blowing snow particles. The strong variation with particle size of this correction implies that the use of detectors with relatively wide scattering acceptance angles can enhance the variation of the effective extinction efficiency with particle size. This variation permits the

use of extinction meters in particle size determiniation as well as drift density measurement.

The theoretical calibration of a particle detector is complex, because the sampling area varies with particle size, particle trajectories diverge from the beam centre resulting in smaller intercepted particle radii and no transmittance level is uniquely associated with an intercepted radius. The identification of a particle size from its individual transmittance is therefore unlikely. However, when large numbers of particles are considered, the number of particles greater than some threshold can be accurately estimated. This value with the extinction coefficient measured by an extinction meter is used to solve for the particle size distribution parameters. With the size distribution solved, the drift density can be precisely calculated. Thus the optical detection system presented here can measure both the quantity and size of blowing snow particles. These parameters are useful in calculating visible range, transport rates and sublimation rates in blowing snow.

REFERENCES

Budd, W.F. 1966. The drifting of non-uniform snow particles. Stud. Antarctic Meteorol., Am. Geophys. Union, Antact. Res. Ser., 9:59-70.

Budd, W.F., W.R.J. Dingle and U. Radok. 1966. The Byrd snow drift project: Outline and basic results. Stud. Antarctic Meteorol., Am. Geophys. Union, Antarct. Res. Ser., 9:71-134.

Haan, C.T. 1977. Statistical Methods in Hydrology. The Iowa State University Press, Ames, Iowa. 378 p.

Hodkinson, J.R. and I. Greenleaves. 1963. Computations of light-scattering and extinction by spheres according to diffraction and geometrical optics, and some comparisons with the Mie theory. J. Opt. Soc. Am., 53(5):577-588.

Irvine, W.M. and J.B. Pollack. 1968. Infrared optical properties of water and ice spheres. Icarus. 8:324-360.

Landon-Smith, I.H. and B. Woodberry. 1965. The photoelectric metering of wind-blown snow. ANARE Interim Reports, Ser.A(IV), 79. Antarct. Div., Dept. of Ext. Affairs, Melbourne. pp. 1-17.

Mellor, M. 1966. Light scattering and particle aggregation in snow-storms. J. Glaciol., 6(44):237-248.

Middleton, W.E.K. 1952. Vision Through the Atmosphere. Toronto, Univ. of Toronto Press. 250 p.

Nussenzveig, H.M. and W.J. Wiscombe. 1980. Efficiency factors in Mie scattering. Phys. Rev. Lettrs., 45(18):1490-1494.

Pomeroy, J.W., T. Brown and D.H. Male. 1985. Measurement of blowing snow properties using optical attenuation devices. Proceedings, Snow Property Measurement Workshop/Symposium. Ottawa. N.R.C.C. Snow and Ice Subcomm. Tech. Mem.

Schmidt, R.A. 1981. Estimates of threshold windspeed from particle sizes in blowing snow. Cold Reg. Sci. Technol., 4:187-193.

Schmidt, R.A. 1982. Vertical profiles of wind speed, snow concentration and humidity in blowing snow. Boundary Layer Meteorol., 23:223-246.

Schmidt, R.A. 1984. Measuring particle size and snowfall intensity in drifting snow. Cold Reg. Sci. Technol., 9:121-129.

Schmidt, R.A., R. Meister and H. Gubler. 1984. Comparison of snow drifting measurements at an alpine ridge crest. Cold Reg. Sci. Technol., 9:131-141.

Seagraves, M.A. 1984. Precipitation rate and extinction in falling snow. J. Atmos. Sci., 41(11):1827-1835.

Tabler, R.D. 1984. Using visual range data for highway operations in blowing snow. Opt. Eng., 23(1):55-61.

Ungut, A., G. Grehan and G. Gouesbet. 1981. Comparisons between geometrical optics and Lorenz-Mie theory. Appl. Opt., 20(17):2911-2918.

van de Hulst, H.C. 1957. Light Scattering by Small Particles. John Wiley and Sons, New York. 470 p.

Wiscombe, W.J. 1980. Improved Mie scattering algorithms. Appl. Opt., 19(9):1505-1509.

Zuev, V.E. 1970. Propagation of Visible and Infrared Radiation in the Atmosphere. Trans. by D. Lederman. Israel Programme for Scientific Translations, London. 405 p.